

# Constraints on variations of $m_p/m_e$ based on UVES observations of $H_2$

M. Wendt<sup>1,\*</sup>

Institute of Physics and Astronomy, University Potsdam, 14476 Potsdam, Germany

Received 30 Aug 2013, accepted Jan 2014

Published online later

**Key words** cosmology: observations, quasars: absorption lines, early universe.

This article summarizes the latest results on the proton-to-electron mass ratio  $\mu$  derived from  $H_2$  observations at high redshift in the light of possible variations of fundamental physical constants. The focus lies on UVES observations of the past years as enormous progress was achieved since the first positive results on  $\Delta\mu/\mu$  were published. With the better understanding of systematics, dedicated observation runs, and numerous approaches to improve wavelength calibration accuracy, all current findings are in reasonable good agreement with no variation and provide an upper limit of  $\Delta\mu/\mu < 1 \times 10^{-5}$  for the redshift range of  $2 < z < 3$ .

© 2014 WILEY-VCH Verlag GmbH & Co. KGaA, Weinheim

## 1 Introduction

The Standard Model of particle physics contains several fundamental constants whose values cannot be predicted by theory and need to be measured through experiments (Fritzsch 2009). These are the masses of the elementary particles and the dimensionless coupling constants which are assumed time-invariant although in theoretical models which seek to unify the four forces of nature they vary naturally on cosmological scales. The fine-structure constant  $\alpha \equiv e^2/(4\pi\epsilon_0\hbar c)$  and the proton-to-electron mass ratio,  $\mu = m_p/m_e$  are two constants that can be probed in the laboratory as well as in the Universe by means of observations of absorption lines due to intervening systems in the spectra of distant quasars (QSO<sup>1</sup>) and have been subject of numerous studies. The former is related to the electromagnetic force while the latter is sensitive primarily to the quantum chromodynamic scale (see, i.e., Flambaum 2004).

In principle, the  $\Lambda_{\text{QCD}}$  scale should vary considerably faster than that of quantum electrodynamics  $\Lambda_{\text{QED}}$ . Consequently, the change in the proton-to-electron mass ratio, if any, should be larger than that of the fine structure constant. Hence,  $\mu$  is an ideal candidate to search for possible cosmological variations of the fundamental constants.

A probe of the variation of  $\mu$  could be obtained by comparing relative frequencies of the electro-vibro-rotational lines of  $H_2$  as first applied by Varshalovich & Levshakov (1993) after Thompson (1975) proposed the general approach to utilize molecule transitions for  $\mu$ -determination. The original paper by Thompson (1975) did not take into account the different sensitivities within the molecular bands, which is the key of the modern approach. The method is based on the fact that the wavelengths of vibro-rotational

lines of molecules depend on the reduced mass,  $M$ , of the molecule. For molecular hydrogen  $M = m_p/2$  so that the comparison of an observed vibro-rotational spectrum at high redshift with its present analog will give information on the variation of  $m_N$  and  $m_e$ . Comparing electro-vibro-rotational lines with different sensitivity coefficients gives a measurement of  $\mu$ .

The observed wavelength  $\lambda_{\text{obs},i}$  of any given line in an absorption system at the redshift  $z$  differs from the local rest-frame wavelength  $\lambda_{0,i}$  of the same line in the laboratory according to the relation

$$\lambda_{\text{obs},i} = \lambda_{0,i}(1+z) \left( 1 + K_i \frac{\Delta\mu}{\mu} \right), \quad (1)$$

where  $K_i$  is the sensitivity coefficient of the  $i$ th component computed theoretically for the Lyman and Werner bands of the  $H_2$  molecule (Meshkov et al. 2007, Ubachs et al. 2007). Figure 1 plots these sensitivity coefficient  $K_i$  for the Lyman<sup>2</sup> and Werner transitions of  $H_2$  in the upper panel. The coefficients are typically on the order of  $10^{-2}$ , some coefficients differ in sign, which means that under the assumption of positive variation of  $\mu$ , some  $H_2$  lines are shifted into opposite directions. The lower panel demonstrates this effect according to equation 1. The shifts for a strongly exaggerated  $\Delta\mu/\mu$  of six lines are shown. The corresponding sensitivity coefficients are marked as *red circles* in the upper panel. The expected shifts at the current level of the constraint on  $\Delta\mu/\mu$  are on the order of a few  $100 \text{ m s}^{-1}$  or about  $1/10^{\text{th}}$  of a pixel size.

It is useful to measure variations in velocities with comparison to the redshift of a given system defined by the red-

\* Corresponding author. e-mail: mwendt@astro.physik.uni-potsdam.de

<sup>1</sup> Historically from 'quasi stellar objects'.

<sup>2</sup> The first digit of an  $H_2$  identifier indicates a Lyman or Werner line, followed by the vibrational quantum number of the excited state and the branch with the rotational number, also referred to as  $J$ .

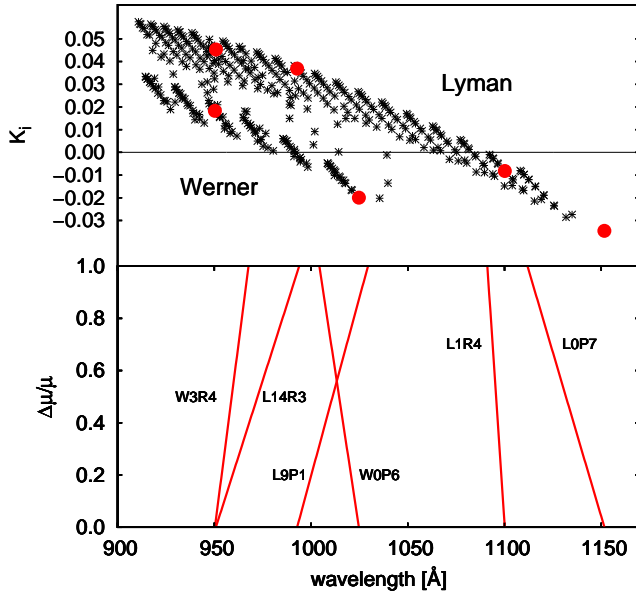


**Fig. 1** The upper panel shows the sensitivity coefficients  $K_i$  of the Lyman and Werner transitions of  $\text{H}_2$  against the restframe wavelength. Note, that the coefficients show different signs. The lower panel demonstrates the shifts of six selected transitions (marked with large red circles in the upper panel) with increasing  $\Delta\mu/\mu$ . The transitions referred to as L9P1 and W0P6 even swap their positions in the observed spectra with increasing  $\Delta\mu/\mu$ . For this illustration the range of  $\Delta\mu/\mu$  is five orders of magnitude larger than the current constraints on  $\Delta\mu/\mu$  (see section 5).

shift position of the lines with  $K_i \approx 0$ , then introducing the reduced redshift  $\zeta_i$ :

$$\zeta_i \equiv \frac{z_i - z}{1 + z} = K_i \frac{\Delta\mu}{\mu}. \quad (2)$$

The velocity shifts of the lines are linearly proportional to  $\Delta\mu/\mu$  which can be measured through a regression analysis in the  $\zeta_i - K_i$  plane. This approach is referred to as line-by-line analysis in contrast to the comprehensive fitting method (CFM). The validity of these two approaches depends mostly on the analyzed  $\text{H}_2$  system. For example, the absorption in QSO 0347-383 (see Wendt & Molaro 2012) has the particular advantage of comprising a single velocity component, which renders observed transitions independent of each other and allow for this regression method. This was also tested in Rahmani et al. (2013) and King et al. (2008). For absorption systems with two or more closely and not properly resolved velocity components many systematic errors may influence distinct wavelength areas. The CFM fits all  $\text{H}_2$  components along with additional H I lines and introduces an artificially applied  $\Delta\mu/\mu$  as free parameter in the fit. The best matching  $\Delta\mu/\mu$  is then derived via the resulting  $\chi^2$  curve. The CFM aims to achieve the lowest possible reduced  $\chi^2$  via additional velocity components. In this approach, the information of individual transitions is lost because merely the overall quality of the comprehensive model is judged. Weerdenburg et al. (2011) increased

the number of velocity components as long as the composite residuals of several selected absorption lines differ from flat noise. As pointed out by King et al. (2011), for multi-component structures with overlapping velocity components the errors in the line centroids are heavily correlated and a simple  $\chi^2$  regression is no longer valid. The same principle applies for co-added spectra with relative velocity shifts. The required re-binning of the contributing data sets introduces further auto-correlation of the individual 'pixels'. Rahmani et al. (2013) discuss the assets and drawbacks of these two approaches in greater detail and find evidence for an unresolved additional velocity component in the spectra for the QSO with the identifier HE 0027 which renders the CFM favorable for that system. The selection criteria for the number of fitted components are non-trivial and under debate. Prause & Reimers (2013) discuss the possibility of centroid position shifts due to incorrect line decompositions with regard to the variation of the finestructure constant  $\alpha$ , which in principle is applicable to any high resolution absorption spectroscopy. The uncertainties of the oscillator strengths  $f_i$  that are stated to be up to 50% (Weerdenburg et al. 2011) might further affect the choice for additional velocity components. Another source of deficient fits may be traced back to the nature of the bright background quasar which in general is not a point-like source. In combination with the potentially small size of the absorbing clumps of  $\text{H}_2$ , we may observe saturated absorption profiles with non negligible residual flux of quasar light not bypassing the  $\text{H}_2$  cloud (see Ivanchik et al. 2011).

## 2 Observations of extragalactic $\text{H}_2$

Molecular hydrogen is the most abundant molecule in the universe and plays a fundamental role in many astrophysical contexts. It is found in all regions where the shielding of the ultraviolet photons, responsible for the photo-dissociation of  $\text{H}_2$ , is sufficiently large. Whenever  $\text{H}_2$  is observed, it traces clumps of molecular hydrogen in galaxies, such as the MilkyWay (Savage et al. 1977) or regions nearby galaxies such as the Small Magellanic Cloud (SMC) or LMC (see, e.g., Richter et al. 1998; deBoer et al. 1998). Observable amounts of  $\text{H}_2$  can only be detected in the H I disks of galaxies as pictured in Figure 2 or in the the so-called Circum-Galactic Medium (CGM).

Except in the very early universe, most  $\text{H}_2$  is likely to be produced via surface reactions on interstellar dust grains, since gas-phase reactions are too slow in general (see, e.g., Harbart et al. 2004). The  $\text{H}_2$  formation mechanism is not yet fully understood. Direct observations of extragalactic  $\text{H}_2$  are difficult since electronic transitions occur only in the ultraviolet and mere roto-vibrational transitions are forbidden due to the homo-nuclear nature of  $\text{H}_2$ . This limits observations to absorption systems at redshifts 2 to 3, for which the absorption features are shifted into the optical. Another problem is the narrow range of conditions under which  $\text{H}_2$  is formed. The required dust grains that allow for

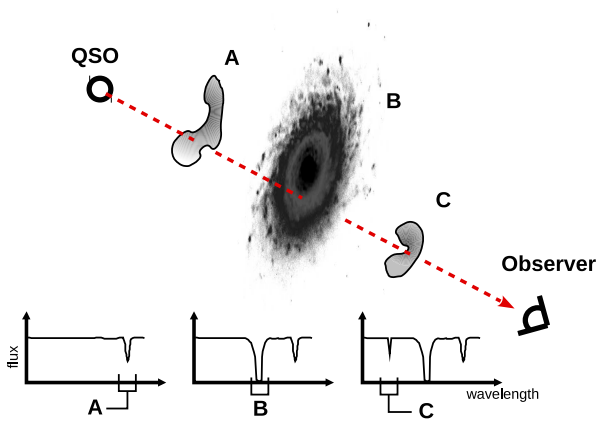


**Fig. 2** Exemplary schematic for the line of sight of an observed quasar. The absorbers A, B and C are passed at decreasing redshift, respectively, and hence leave their signature at different redshifted wavelengths in the observed spectrum. At B the line of sight pierces a dense part of a galaxy with more than  $2 \times 10^{20}$  atoms/cm<sup>2</sup> integrated, a so-called damped Ly- $\alpha$  (DLA) system. Only here extragalactic H<sub>2</sub> can be detected under special conditions.

the forming of H<sub>2</sub> can easily obscure the molecular hydrogen as well.

There are very few comprehensive studies on the spatial distribution of H<sub>2</sub> in intervening absorption systems. Hirashita et al. (2003) computed the H<sub>2</sub> distribution based on the ultraviolet background (UVB) intensity and dust-to-gas ratios and find that H<sub>2</sub> has a very inhomogeneous, clumpy distribution on sub-parsec scale which explains the low number of known extragalactic H<sub>2</sub> absorbers.

Only a small fraction of observable lines of sight through DLAs cross these isolated regions (as illustrated in Figure 2). The Lyman bands in the wavelength range between 1000 Å and 1100 Å were first identified in the absorption spectrum of a diffuse interstellar cloud in the optical path towards  $\xi$  Persei (Carruthers et al. 1970). Further spaceborne observations also revealed absorption of Werner bands and UV emission of Lyman and Werner bands including their continua (Spitzer et al. 1974). Levshakov et al. (1985) tentatively assigned some features in spectra obtained by Morton et al. (1980) from PKS 0528-250 (one of the few systems up to date used for determination of  $\mu$ , see table 1). Additional data of this system were taken and used for a first constraint on a possible variation of  $\mu$  put forward by Varshalovich & Levshakov (1993). Observations with the Ultraviolet and Visual Echelle Spectrograph (UVES) at the Very Large Telescope (VLT) in Paranal, Chile, led to H<sub>2</sub> detections towards QSO 0347-383, QSO 1232+082 (Ivanchik et al. 2002; Levshakov et al. 2002), and towards QSO 0551-336 (Ledoux et al. 2002). Additional observations of H<sub>2</sub> are reported towards Q 0000-263 in Levshakov et al. (2000). Ledoux et al. (2003) and Srikanand et al. (2005) performed surveys on DLA systems at redshifts  $z > 1.8$ , in

**Table 1** List of damped Lyman- $\alpha$  systems with H<sub>2</sub> absorption observations with  $z > 2$ .

Quasar source	redshift $z_{\text{abs}}$	comment
J 2123-005	2.06	$\Delta\mu/\mu$ measured
Q 1444+014	2.09	
Q 1232+082	2.34	H <sub>2</sub> saturated
Q 0841+129	2.37	H <sub>2</sub> very weak
Q 1439+113	2.42	
Q 2348-011	2.42	$\Delta\mu/\mu$ measured
HE 0027-184	2.42	$\Delta\mu/\mu$ measured
Q 2343+125	2.43	H <sub>2</sub> very weak
Q 0405-443	2.59	$\Delta\mu/\mu$ measured
FJ 0812+320	2.63	northern target
Q 0642-506	2.66	$\Delta\mu/\mu$ measured
J 1237+064	2.69	
Q 0528-250	2.81	$\Delta\mu/\mu$ measured
Q 0347-383	3.02	$\Delta\mu/\mu$ measured
Q 1337+315	3.17	H <sub>2</sub> very weak
Q 1443+272	4.22	northern target

which some new quasars with H<sub>2</sub> absorption were detected. Later on, Petitjean et al. (2006) observed the DLA systems in QSO 2343+125 and QSO 2348-011, while Ledoux et al. (2006) observed H<sub>2</sub> lines in a spectrum at the highest redshift to date with  $z = 4.22$ . In the course of the 'UVES Large Program for testing fundamental physics' numerous QSOs were observed between 2010 and 2013 with the intention to exploit the capabilities of the instrument and to achieve the best possible constraints and variations of  $\alpha$  and  $\mu$  (see Molaro et al. 2013; Rahmani et al. 2013). Noterdaeme et al. (2008) concluded from the comparison between H<sub>2</sub>-bearing systems and the overall UVES sample, that a significant increase of the molecular fraction in DLAs could take place at redshifts  $z_{\text{abs}} \geq 1.8$ . The known DLA systems with H<sub>2</sub> absorption in the redshift range observable with UVES and suitable for the determination of  $\Delta\mu/\mu$  are listed in Table 1.

### 3 Wavelength calibration for UVES

In recent years the wavelength calibration emerged to be one of the most relevant aspects in modern high resolution spectroscopy in particular for fields with such an accentuated interest in line positions. The error budget of the calibration is most difficult to estimate and its nature in some aspects still unknown. Most high resolution UVES observations of QSOs for this purpose are taken with a slit width around 0.8'' providing a resolving power in the order of  $\lambda/\Delta\lambda \approx 60\,000^3$ . This value is to be understood as a rough estimate of the expected resolution as the resolving power varies by up to 20 % along individual wavelength orders (see Wendt & Molaro 2012). The pixel-wavelength-conversion of the wavelength calibration is done by using the corresponding

<sup>3</sup> The resolving power R is not well defined and instrument specific (Robertson 2013).

calibration spectrum. Murphy et al. (2008) and Thompson et al. (2009) independently showed that the standard Th/Ar line list used in older UVES pipelines was the primary limiting factor. The laboratory wavelengths of the calibration spectrum were only given to three decimal places (in units of Å) and, in many cases, the wavelengths were truncated rather than rounded from four decimal places (see Murphy et al. 2007).

Thompson et al. (2009) re-calibrated the wavelength solutions using the calibration line spectra taken during the observations of the QSOs and argued that the new wavelength calibration was a key element in their null result. They describe the whole calibration process for UVES in great detail. In Wendt & Molaro (2012), typical residuals of the wavelength calibrations were  $\sim 0.34 \text{ mÅ}$  or  $\sim 24 \text{ m s}^{-1}$  at  $4000 \text{ Å}$ . Malec et al. (2010) give wavelength calibration residuals of  $\text{RMS} \sim 80 \text{ m s}^{-1}$  for KECK/HIRES, and Rahmani et al. (2013) obtained an average error of the wavelength solution of  $\sim 40\text{-}50 \text{ m s}^{-1}$  which is the expected range for the UVES pipeline and ThAr lamp based calibration in general. However, this error estimate only accounts for the statistical aspect of the wavelength calibration. Intrinsic systematics cannot be identified that easily. Only calibration lamp exposures taken immediately before and after object observations provide an accurate monitoring of the physical conditions. Moreover, the calibration frames were taken in special mode to avoid automatic spectrograph resetting at the start of every exposure. Since Dec 2001 UVES has implemented an automatic resetting of the Cross Disperser encoder positions at the start of each exposure. This implementation has been done to have the possibility to use daytime ThAr calibration frames for saving night time. If this is excellent for standard observations, it is a problem for the measurement of fundamental constants which requires the best possible wavelength calibration. Additionally, thermal-pressure changes move in the cross dispersers in different ways, thus introducing relative shifts between the different spectral ranges in different exposures. There are no measurable temperature changes for the short exposures of the calibration lamps but during the much longer science exposures the temperature drifts generally by  $\leq 0.2 \text{ K}$ . The estimates for UVES are of  $50 \text{ m s}^{-1}$  for  $\Delta T = 0.3 \text{ K}$  or a  $\Delta P = 1 \text{ mbar}$  (Kaufer et al. 2004), thus assuring a radial velocity stability within  $\sim 50 \text{ m s}^{-1}$ . The motion of Earth during observation smears out the line by  $\pm 40 \text{ m s}^{-1}$ , since the line shape itself remains symmetric, this does not directly impact the centroid measurements but it will produce an absorption profile that is no longer strictly Gaussian (or Voigt) but rather slightly squared-shaped which further limits the quality of a line fit and must be considered for multi-component fits of high resolution spectra.

The measured air wavelengths are commonly converted to vacuum via the dispersion formula by Edlen (1966). Drifts in the refractive index of air inside the spectrograph between the ThAr and quasar exposures will therefore cause mis-calibrations. According to the Edlen formula for the re-

fractive index of air, temperature and atmospheric pressure changes of  $1 \text{ K}$  and  $1 \text{ mbar}$  would cause differential velocity shifts in the optical in the order of  $\sim 10 \text{ m s}^{-1}$ .

A stronger concern is the possibility of much larger distortions within the spectral orders which have been investigated at the Keck/HIRES spectrograph by comparing the ThAr wavelength scale with a second one established from I2-cell observations of a bright quasar by Griest et al. (2010). They find absolute offsets which can be as large as  $500 - 1000 \text{ m s}^{-1}$  and an additional distortion of about  $300 \text{ m s}^{-1}$  within the individual orders. The distortion is such that transitions at the edges of the Echelle orders appear at different velocities with respect to transitions at the order centers when calibrated with a ThAr exposure. This would introduce relative velocity shifts between different absorption features up to a magnitude the analysis with regard to  $\Delta\mu/\mu$  is sensitive to. Whitmore et al. (2010) repeated the same test for UVES with similar results though the distortions fortunately show lower peak-to-peak velocity variations of  $\sim 200 \text{ m s}^{-1}$ , and Wendt & Molaro (2012) detected indications for this effect directly in the measured positions of  $\text{H}_2$  features as well.

Molaro et al. (2011) suggested to use the available solar lines atlas in combination with high resolution asteroid spectra taken close to the QSO observations to check UVES interorder distortions and published a revised solar atlas in Molaro & Monai (2012). Such asteroid spectra were used as absolute calibration to determine velocity drifts in their data via cross-correlation of individual wavelength intervals in Rahmani et al. (2013). They found distinct long range drifts of several  $100 \text{ m s}^{-1}$  within  $1000 \text{ Å}$ . The origin of these drifts remains currently unknown but is verified in Whitmore et al. (2013 in prep.) and considered by Bagdonaite et al. (2013) to contribute to their positive signal. Rahmani et al. (2013) found the drift to be constant over a certain epoch and applied suitable corrections. So far the drift, when present, in UVES spectra always showed the same trend at different magnitudes which could be an explanation for the reported tendency towards positive variation in  $\mu$  (see section 5).

## 4 Determination of precise line centroids

Table 1 lists all extragalactic  $\text{H}_2$  features in DLA systems known today that are in principle suitable for  $\Delta\mu/\mu$  measurements. Those already analyzed for the purpose of  $\Delta\mu/\mu$  determination are pointed out in the rightmost column. Q2348-011 shows a quite complex velocity structure in  $\text{H}_2$  including detected self-blending which is partially reflected in the comparably large errorbars on this measure (see Bagdonaite et al. 2012). An important benefit from analyzing molecular hydrogen in DLA systems is the large number of observable transitions which lies in the order of  $50\text{-}100$  for the observed systems. Considering the very limited typical size of the dense  $\text{H}_2$  absorbers on the (sub)parsec scale, we are confident that all observed tran-

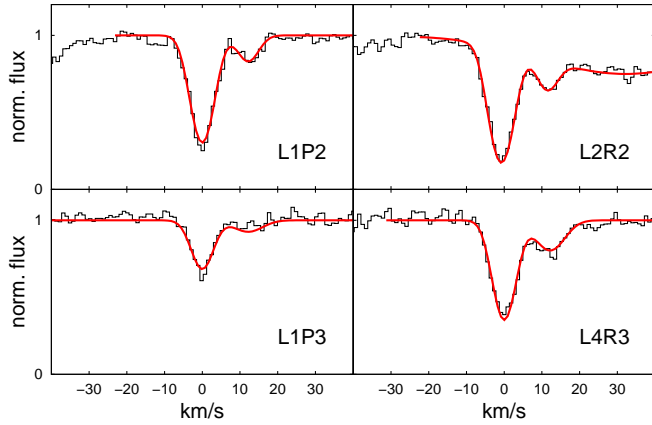


**Fig. 3** Four exemplary  $H_2$  features in QSO 0405-443 to demonstrate the tied fitting parameters. Given in each panel at the lower right is the identifier of the observed transition. An additional broad  $Ly-\alpha$  component was added for L2R2, the  $H_2$  is fitted with two velocity components with a separation of  $12.2 \text{ km s}^{-1}$ . The shown fit is based merely on these four features.

sitions occur in the same physically bound medium. This information can be used in simultaneous fits of all observed  $H_2$  features with tied parameters. In general a common column density is fit to all transitions from the same rotational level. At sufficiently high resolution it becomes mandatory to take into account the possible multiphase nature of different  $J$ -levels as proposed in Noterdaeme et al. (2007) and applied, i.e., in Wendt & Molaro (2012) and Rahmani et al. (2013), who fitted individual line broadening parameters to different  $J$ -levels.

QSO 0405-443 shows a weaker second velocity component which is well resolved. Figure 3 shows four transitions, namely L1P2, L2R2, L1P3, and L4R3. These features were fitted with a common column density for each component in the  $J = 2$  transitions in the panels and one for the  $J = 3$  lines. To each  $J$ -group the  $b$ -parameters per velocity component were coupled and a global velocity separation of both components was fitted to all four lines. The small number of simultaneously fitted lines shows in the lower panel for the second component whose column density for L1P3 was probably overestimated due to some contamination of L4R3. Only for the typically large number of lines per rotational level these effects cancel out. Former studies of QSO 0405 neglected the second component at an offset of about  $12 \text{ km s}^{-1}$  for the analysis of  $\Delta\mu/\mu$  as it is considerably weaker. However, it can be utilized to get a proper measure of the oscillator strengths of the transitions, which are stated to differ notably from the calculated values (see Weerdenburg et al. 2011). For this case the oscillator strengths were allowed to vary by up to 20 % which resulted in improved fits. The additional, resolved second component breaks the degeneracy for limited signal-to-noise data of the column density  $N$ , broadening parameter  $b$ , and oscillator frequency  $f_{\text{osc}}$  as the latter of course is identical for all velocity components. These particular entangled fits are carried out with

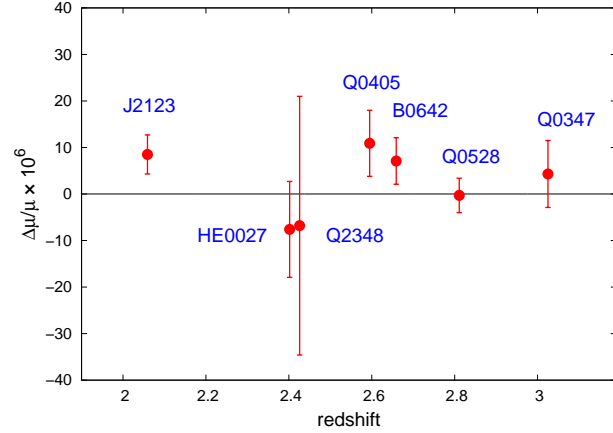


**Fig. 4** Latest results for  $\Delta\mu/\mu$  based on  $H_2$  in seven different quasar sightlines observed with UVES: J2123-0050 (van Weerdenburg et al. 2011), HE0027-1836 (Rahmani et al. 2013), Q2348-011 (Bagdonaite et al. 2012), Q0405-443 (King et al. 2008), B0642-5038 (Bagdonaite et al. 2013), Q0528-250 (King et al. 2011), Q0347-383 (Wendt & Molaro 2012). The given errorbars are the sum of statistical and systematic error (if both are given) under the assumption of gaussian distributed errors.

an evolutionary fitting algorithm, that allows complex links between fitting parameter. The routine is based on Quast, Baade & Reimers (2005) and was verified for this application in Wendt & Reimers (2008). An analysis making use of this additional boundary condition for simultaneous fits is currently in progress (Wendt et al. 2014 in prep.).

## 5 Published results for $\Delta\mu/\mu$ since 2008 based on UVES observations of $H_2$

There were numerous determinations of  $\Delta\mu/\mu$  ever since early indications of change in  $\Delta\alpha/\alpha$  were published and in particular after the paper by Reinhold et al. (2006) who presented evidence that the proton-to-electron mass ratio was larger in the past at the  $> 3.5\sigma$  level. Several inconsistencies between different analyses for  $\Delta\mu/\mu$  and  $\Delta\alpha/\alpha$  surfaced until it became evident that systematic errors were responsible for the large scatter in the results. The following Table 1 lists publications that determined  $\Delta\mu/\mu$  based on observations of  $H_2$  at high redshift with UVES. For clarity, only works since 2009 (with one exception) are listed. This also rectifies the situation of cited earlier results that likely were dominated by the mentioned systematics in the wavelength calibration and limited accuracy of the rest-frame wavelengths as well as insufficient data quality. King et al. (2008) is added to the list since they determined the latest published value for  $\Delta\mu/\mu$  for QSO 0405-443, which is currently being re-analyzed. The value for  $\Delta\mu/\mu$  based on J 2123-0050 in van Weerdenburg et al. (2011) was preceded by Malec et al. (2010) who observed the same system with the KECK telescope. Both results are in reasonable good

agreement. The publications in the table are sorted by the time the data were taken, which is loosely correlated to the data quality with regard to the calibration preparations and general high resolution and signal-to-noise requirements for the purpose of probing fundamental physics.

Figure 4 shows the latest measurements of  $\Delta\mu/\mu$  based on  $\text{H}_2$  observations with UVES for 7 observed quasar spectra. Bagdonaite et al. (2013) raise the point that they found evidence based on asteroid observations for a possible long range distortion of about  $350 \text{ m s}^{-1}$  over  $1000 \text{ \AA}$  in their observations of B0642, a systematic that would translate to an offset in  $\Delta\mu/\mu$  of  $-10 \times 10^{-6}$ . The analyzed asteroid spectra, however, were not taken during the observations of the quasar and hence were not applied as correction. The presented data of seven measurements yields a mean of  $\Delta\mu/\mu = (3.7 \pm 3.5) \times 10^{-6}$  and is in good agreement with a non-varying proton-to-electron mass ratio<sup>4</sup>. Such a generic mean value does not take into account any interpretation with regard to spatial or temporal variation and instead merely evaluates the competitive data available for  $\Delta\mu/\mu$  based on  $\text{H}_2$ -observations, which consequently are limited to the redshift range of  $2 < z_{\text{abs}} < 3$  and the evidence these data provide for any non constant behavior of  $\mu$  over redshift. This tight constraint already falsifies a vast number of proposed theoretical models for varying  $\mu$  or  $\alpha$ . Thompson et al. (2013) come to the conclusion that that “adherence to the measured invariance in  $\mu$  is a very significant test of the validity of any proposed cosmology and any new physics it requires”.

Current efforts to  $\Delta\mu/\mu$  measurements exploit the technical limits of the UVES spectrograph and bring forward valuable new aspects of quasar absorption system analysis. The data from the ESO LP<sup>5</sup> observations has the potential to set a new cornerstone in the assessment of variability of fundamental physical constants. Observations featuring instruments in the foreseeable future will provide further insights and allow to bring cosmological measurements of intergalactic absorbers into a new era. Spectra recorded via laser-comb calibrated spectrographs (such as CODEX or EXPRESSO) at large telescopes (E-ELT or VLT, respectively) implicate new methods of data analysis as well. High resolution spectroscopy gains importance in several fields. The next generation of instruments, such as the Potsdam Echelle Polarimetric and Spectroscopic Instrument (PEPSI) designed for the at the Large Binocular Telescope (LBT) features resolutions of up to 310000 (Strassmeier et al. 2008) and will already require improvements of absorption line modeling from simple symmetric Voigt-profiles to more physical models incorporating intrinsic velocity structures and inhomogeneities of the absorber.

*Acknowledgements.* We appreciate the cooperation with the authors of AN and are thankful for the organizers of the 10<sup>th</sup> Potsdam Thinkshop on ‘High resolution optical spectroscopy’ which

<sup>4</sup> If the mentioned correction is applied, this changes to  $\Delta\mu/\mu = (2.3 \pm 2.8) \times 10^{-6}$ .

<sup>5</sup> ESO telescope program L185.A-0745

motivated this article on the status quo. We further want to express our gratitude to Philipp Richter and Helge Todt for helpful comments and discussions.

## References

- Bagdonaite, J., Murphy, M. T., Kaper, L., Ubachs, W. 2012, MNRAS, 421, 419-425
- Bagdonaite, J., Ubachs, W., Murphy, M. T., Whitmore, J. B. 2013, ApJ submitted arXiv:1308.1330v1
- Carruthers, G. R. 1970, ApJ, 161, 81
- de Boer, K. S., Richter, P., Bomans, D. J., Heithausen, A., Koornneef, J., 1998, A&A, 338, 5-8
- Edlén, B. 1966, Metrologia, 2, 71
- Flambaum, V. V., Leinweber, D. B., Thomas, A. W., Young, R. D. 2004, Phys. Rev. D, 69
- Fritzsche, H. 2009, Physics-Uspekhi, 52, 359
- Griest, K., Whitmore, J. B., Wolfe, A. M., et al. 2010, ApJ, 708, 158
- Habart, E., Boulanger, F., Verstraete, L., Walmsley, C. M., Pineau des Forêts, G. 2004, A&A, 414, 531-544
- Hirashita, H., Ferrara, A., Wada, K., Richter, P. 2003, MNRAS, 341, L18-L22
- Ivanchik, A. V., Rodriguez, E., Petitjean, P., Varshalovich, D. A. 2002, Astronomy Letters, 28, 423-427
- Ivanchik, A. V., Petitjean, P., Balashev, S. A., Srianand, R. and Varshalovich, D. A., Ledoux, C., Noterdaeme, P. 2010, MNRAS, 404, 1583-1590
- Kaufer, A., D’Odorico, S., Kaper, et al. 2004, UVES User manual
- King, J. A., Webb, J. K., Murphy, M. T., Carswell, R. F. 2008, Phys. Rev. Lett., 101
- King, J. A., Murphy, M. T., Ubachs, W., Webb, J. K. 2011, MNRAS, 417, 3010
- Ledoux, C., Srianand, R., Petitjean, P. 2002, A&A, 392, 781-789
- Ledoux, C., Petitjean, P., Srianand, R. 2003, MNRAS, 346, 209-228
- Ledoux, C., Petitjean, P., Srianand, R. 2006, ApJ, 640, 25-28
- Levshakov, S. A., Varshalovich, D. A. 1985, MNRAS, 212, 5127-521
- Levshakov, S. A., Molaro, P., Centurión, M., D’Odorico, S., Bonifacio, P., Vladilo, G. 2000, A&A, 361, 803-810
- Levshakov, S. A., Dessauges-Zavadsky, M., D’Odorico, S., Molaro, P. 2002, MNRAS, 333, 373
- Malec, A. L., Buning, R., Murphy, M., et al. 2010, MNRAS, 403, 1541
- Meshkov, V. V., Stolyarov, A. V., Ivanchik, A. V., Varshalovich, D. A. 2006, JETPL, 83, 303
- Molaro, P., Centurión, M. 2011, A&A, 525, 74
- Molaro, P., Monai, S. 2012, A&A, 544, 125
- Molaro, P., Centurión, M., Whitmore, J. B., Evans, T. M., Murphy, M. T., Agafonova, I. I., Bonifacio, P., D’Odorico, S., Levshakov, S. A., Lopez, S., Martins, C. J. A. P., Petitjean, P., Rahmani, H., Reimers, D., Srianand, R., Vladilo, G., Wendt, M. 2013, A&A, 555, A68
- Morton, D. C., Wright, A. E., Peterson, B. A., Jauncey, D. L., Chen, J. 1980, MNRAS, 193, 399-413
- Murphy, M. T., Tzanavaris, P., Webb, J. K., Lovis, C. 2007, MNRAS, 378, 221-230
- Murphy, M. T., Webb, J. K., Flambaum, V. V., et al. 2008, MNRAS, 384, 1053
- Noterdaeme, P., Ledoux, C., Petitjean, P., Le Petit, F., Srianand, R., Smette, A. 2007, A&A, 474, 393-407

**Table 1**  $\Delta\mu/\mu$  measurements based on H<sub>2</sub> observations with VLT/UVES.

Reference	object	data	redshift	$\Delta\mu/\mu \times 10^{-6}$	comment
King et al. (2008)	QSO 0405-443	(2002)	2.595	$10.9 \pm 7.1$	data from earlier analyses new calibration applied
Thompson et al. (2009)	QSO 0347-383	(2002)	3.025	$-28 \pm 16$	thorough new calibration ThAr linelist renewed
Wendt & Molaro (2011)	QSO 0347-383	(2002,2003)	3.025	$15.0 \pm 10.8$	utilizing independent data from 2003 to gain robustness
Ubachs et al. (2011)	QSO 2348-011	(2007)	2.426	$-15 \pm 16$	non-ideal data improved in 2013
Malec et al. (2010)	J 2123-0050	(2007)	2.059	$5.6 \pm 6.2$	based on KECK data
van Weerdenburg et al. (2011)	J 2123-0050	(2008)	2.059	$8.5 \pm 4.2$	based on UVES data
Bagdonaite et al.(2012)	QSO 2348-011	(2008)	2.426	$-6.8 \pm 27.8$	complex H <sub>2</sub> system refined analysis
Bagdonaite et al.(2013)	B 0642-5038	(2004,2008)	2.659	$17.1 \pm 5.0$	result possibly influenced by long range drift
King et al. (2011)	QSO 0528-250	(2008,2009)	2.811	$-0.3 \pm 3.7$	re-observation due to slit and calibration issues in former analysis, H <sub>2</sub> and HD detected
Wendt & Molaro (2012)	QSO 0347-383	(2009)	3.025	$4.3 \pm 7.2$	re-observation to exploit UVES capabilities, LP specifications
Rahmani et al. (2013)	HE 0027-1836	(2010-2012)	2.402	$-7.6 \pm 10.3$	LP data, quantitative determi- nation of long range drift

- Noterdaeme, P., Ledoux, C., Petitjean, P., Srianand, R., A&A, 481, 327-336
- Petitjean, P., Ledoux, C., Noterdaeme, P., Srianand, R., A&A, 456, 9-12
- Prause, N., Reimers, D. 2013, A&A, 555, 88
- Quast, R., Baade, R., Reimers, D. 2005, ApJ, 431, 1167
- Rahmani, H., Wendt, M., Srianand, R., Noterdaeme, P., Petitjean, P., Molaro, P., Whitmore, J. B., Murphy, M. T., Centurion, M., Fathivavari, H., D'Odorico, S., Evans, T. M., Levshakov, S. A., Lopez, S., Martins, C. J. A. P., Reimers, D., Vladilo, G. MNRAS in press arXiv:1307.5864v1
- Reinhold, E., Buning, R., Hollenstein, U., et al. 2006, Phys. Rev. Lett., 96, 15
- Richter, P., Widmann, H., de Boer, K. S., Appenzeller, I., Barnstedt, J., Golz, M., Grewing, M., Gringel, W., Kappelmann, N., Kramer, G., Mandel, H., Werner, K. 1998, A&A, 338, 9-12
- Robertson, J. G. 2013, arXiv:1008.3907
- Savage, B. D., Bohlin, R. C., Drake, J. F., Budich, W. 1977, ApJ, 216, 291-307
- Spitzer, Jr., L., Cochran, W. D., Hirshfeld, A. 1974, ApJ, 28, 373-389
- Srianand, R., Petitjean, P., Ledoux, C., Ferland, G., Shaw, G. 2005, MNRAS, 362, 549-568
- Strassmeier, K. G., Woche, M., Ilyin, I., Popov, E., Bauer, S.-M., Dionies, F., Fechner, T., Weber, M. and Hofmann, A., Storm, J., Materne, R., Bittner, W., Bartus, J., Granzer, T., Denker, C., Carroll, T., Kopf, M., DiVarano, I., Beckert, E., Lesser, M. 2008, SPIE, 7014
- Thompson, R. I. 1975, Astrophys. Lett., 16, 3
- Thompson, R. I., Bechtold, J., Black, J. H., et al. 2009, ApJ, 703, 2
- Thompson, R. I., Bechtold, J., Black, J. H., Martins, C. J. A. P. 2009, New A, 14, 379
- Thompson, R. I., Martins, C. J. A. P., Vielzeuf, P. E. 2013, MNRAS, 428, 2232-2240
- Ubachs, W., Buning, R., Eikema, K. S. E., Reinhold, E. 2007, J. Molec. Spec., 241, 155
- Ubachs, W., Bagdonaite, J., Murphy, M. T., Buning, R., Kaper, L. 2011, SPRINGER press arXiv:1101.5150v4
- Varshalovich, D. A., Levshakov, S. A. 1993, JETP, 58, 231
- van Weerdenburg, F., Murphy, M. T., Malec, A. L., Kaper, L., Ubachs, W. 2011, Phys. Rev. Lett., 106, 180802
- Wendt, M., Reimers, D. 2008, EPJ, 163, 197-206
- Wendt, M., Molaro, P. 2011, A&A, 526, 96
- Wendt, M., Molaro, P. 2012, A&A, 541, 69
- Whitmore, J. B., Murphy, M. T., Griest, K. 2010, ApJ, 723, 89